Supporting Information

Towards Optimized Radial Modulation of Space-Charge Region in One-Dimensional SnO_2-NiO Core-Shell Nanowires for Hydrogen Sensing

Muhammad Hamid Raza[1], Navpreet Kaur[2], Elisabetta Comini[2*], Nicola Pinna[1*]

1 -Institut für Chemie and IRIS Adlershof, Humboldt-Universität zu Berlin, Brook-Taylor-Str. 2, 12489 Berlin, Germany

2 - Sensor Lab, Department of Information Engineering, University of Brescia, Via Valotti 9, 25133 Brescia, Italy

* Corresponding Author E-mail: elisabetta.comini@unibs.it, nicola.pinna@hu-berlin.de

The growth of the NiO ALD film was initially monitored by spectroscopic ellipsometry (SE) on the well-cleaned silicon wafers, which were coated in the ALD chamber at the same time as the SnO_2 nanowires. The obtained data were fitted to the optical model using the SpectraRay 4 software. A statistical correlation exists for metal-based thin films between the optical constants and thicknesses when fitting an optical model to the ellipsometric data values.[1] The comparison and the fits of ellipsometric data obtained by the NiO coated silicon wafers and the non-coated silicon wafer confirmed the success of the ALD process. It can be seen, in the data fits, that the curves move consistently to a comparatively lower delta (Δ) values with increasing the number of ALD cycles. The growth per cycle (GPC) was calculated by the slope of the linear fit of the thickness of the NiO film deposited *vs.* the number of ALD cycles on Si/SiO_2 wafers. It shows a linear growth (R^2 = 0.976), evidencing the linear behavior with a growth per cycle (GPC) of 0.37 Å/cycle (**Figure S1b**).

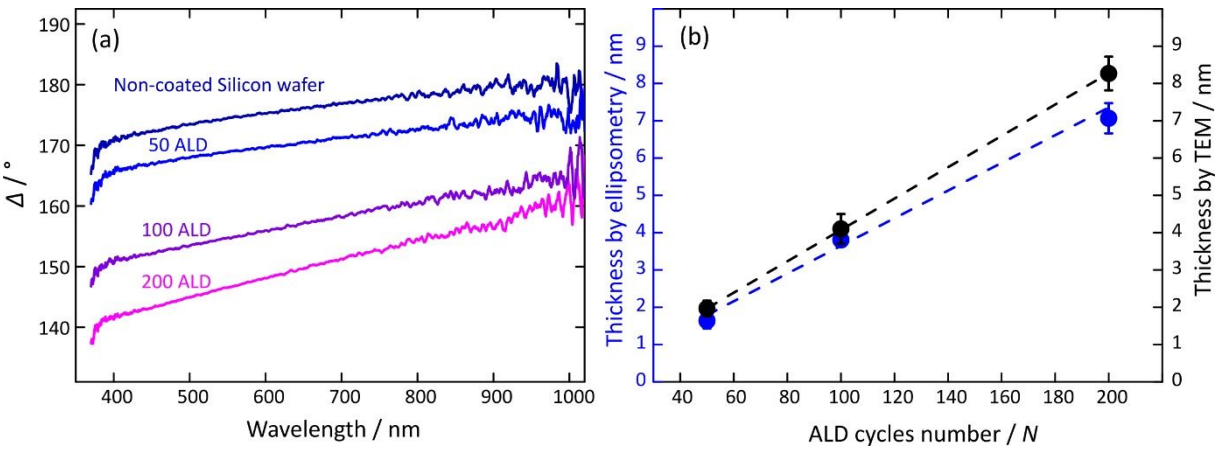

Figure S1. (a) Spectroscopic ellipsometry curves (Delta $\Delta(\lambda)$) for the non-coated and the NiO coated Si/SiO_2 wafers with various numbers of NiO ALD cycles, showing the systematic film thickness increase with increasing the number of ALD cycles, (b) linear fit of the NiO thickness with the number of ALD cycles estimated on the silicon wafers and SnO_2 nanowires by spectroscopic ellipsometry (Blue) and the transmission electron microscopy (Black), respectively.

The crystalline structure of the pristine SnO_2 NWs and SnO_2/NiO-*X* CSNWs was further investigated by GIXRD. The as-synthesized SnO_2 nanowires show a diffraction pattern, which matched-well with the cassiterite phase of SnO_2 (ICDD 00-001-0625). The SnO_2/NiO-*X* samples shows diffraction pattern mainly attributed to the SnO_2 and alumina substrate (**Figure S2**). The XRD peaks of NiO are less pronounced due to the low film thickness (ca. 1.9 8 nm) and the small crystallite sizes. This is consistent to the already reported XRD patterns for the NiO coated carbon nanotubes (NiO/SCCNTs), where the CNTs coated with 25 100 ALD cycles (ca. 0.8 4 nm) showed no clear reflections of the NiO, whereas the sample with 200 ALD cycles showed some week reflections that were assigned to the NiO rock-salt structure.[2,3] Moreover, the most intense 111 and 200 reflections of the rock salt structure overlap with the reflections from SnO_2 and alumina substrate. On the other hand, the peak at 27.8° can be distinguished in the SnO_2/NiO-*200* samples measured at low incident angle, ω=0.5 (ICDD 01-075-0197). The signals marked with asterisks (*) are the background traces by the alumina substrate.

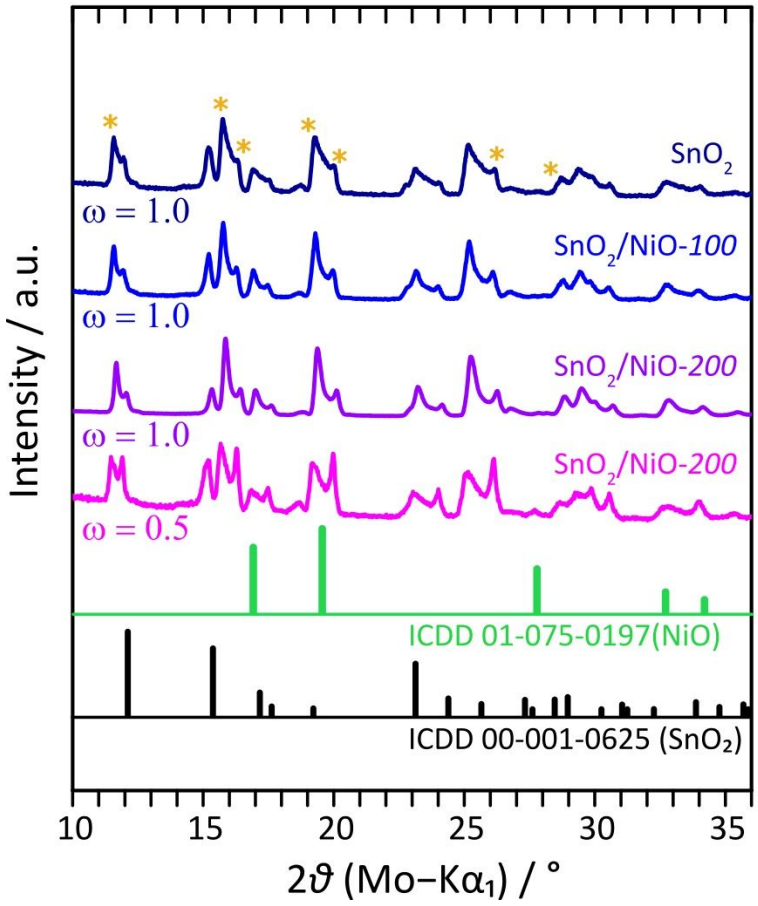

Figure S2. GIXRD traces for the pristine SnO_2 NWs and NiO coated SnO_2 CSNWs with 100 and 200 ALD cycles.

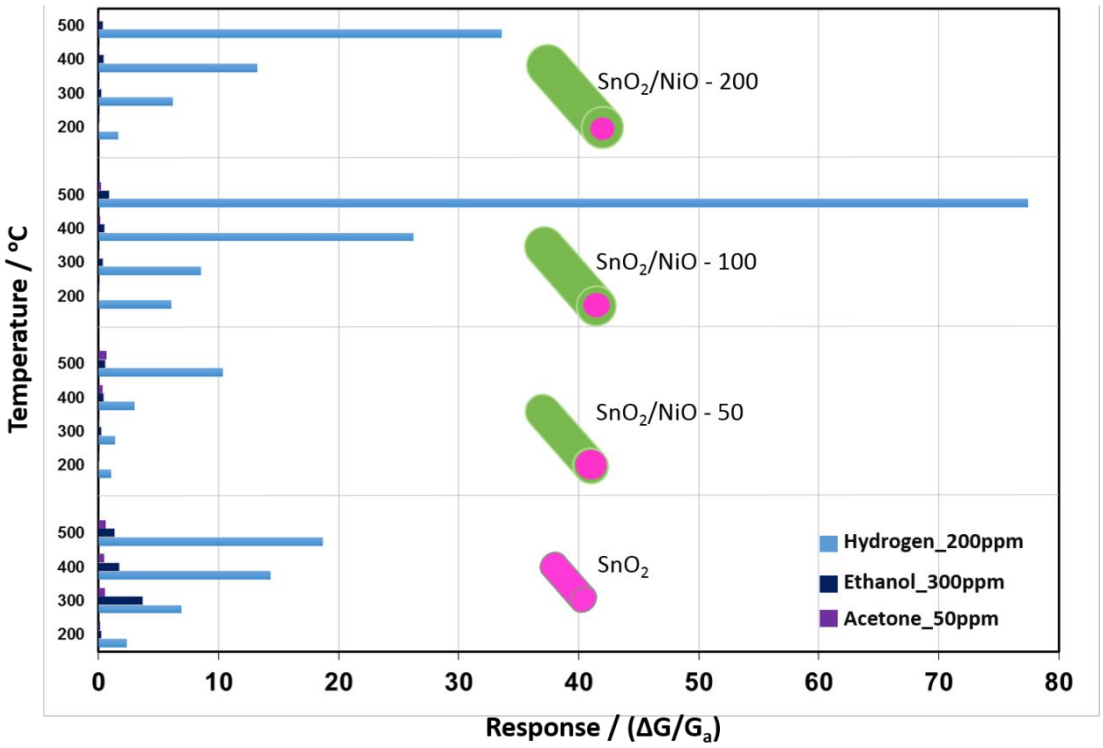

Figure S3. Gas-sensing response of the sensors fabricated with pristine SnO_2 nanowires and SnO_2/NiO-*X* CSNWs heterostructures towards acetone (50 ppm), ethanol (300 ppm) and H_2 (200 ppm) in dry air at various temperatures.

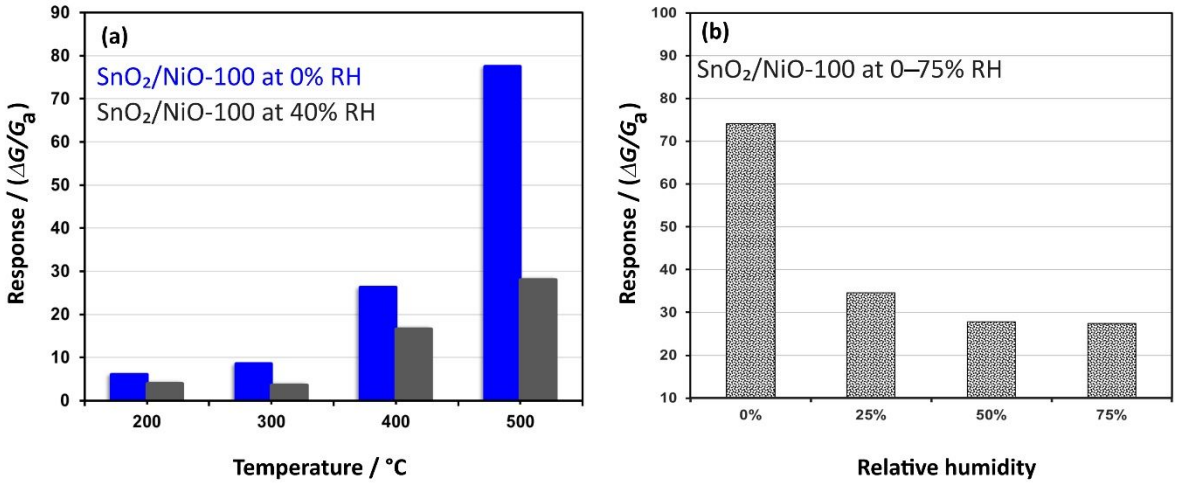

Figure S4. Response of the sensor fabricated with SnO_2/NiO-*100* CSNWs heterostructures towards 200 ppm of hydrogen, (a) at various operating temperatures for the relative humidity levels (RH) of 0% and 40% () and (b) at different humidity levels (RH, 0 75%) for a fixed temperature of 500 °C.

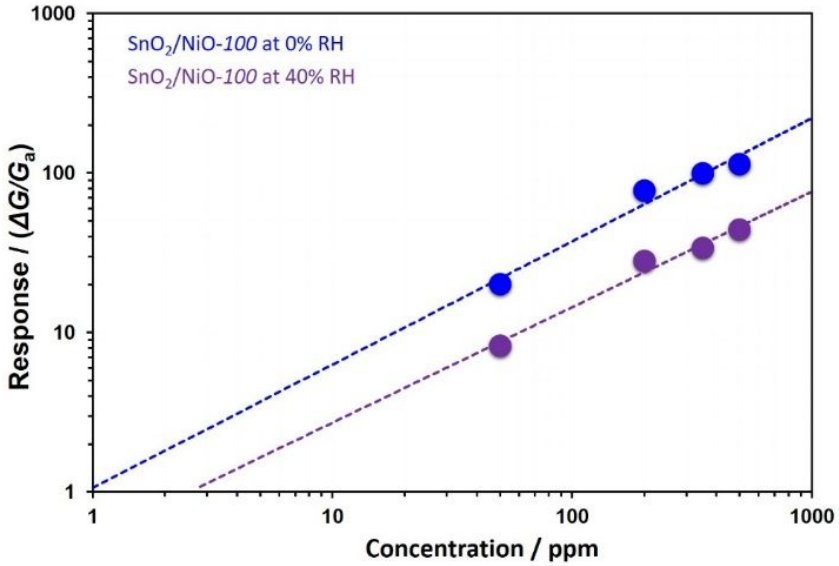

Figure S5. Calibration plots (sensing responses *vs.* hydrogen concentrations) for the sensors fabricated with SnO_2/NiO-*100* CSNWs heterostructures at 0% and 40% relative humidity levels at an optimum temperature of 500 °C.

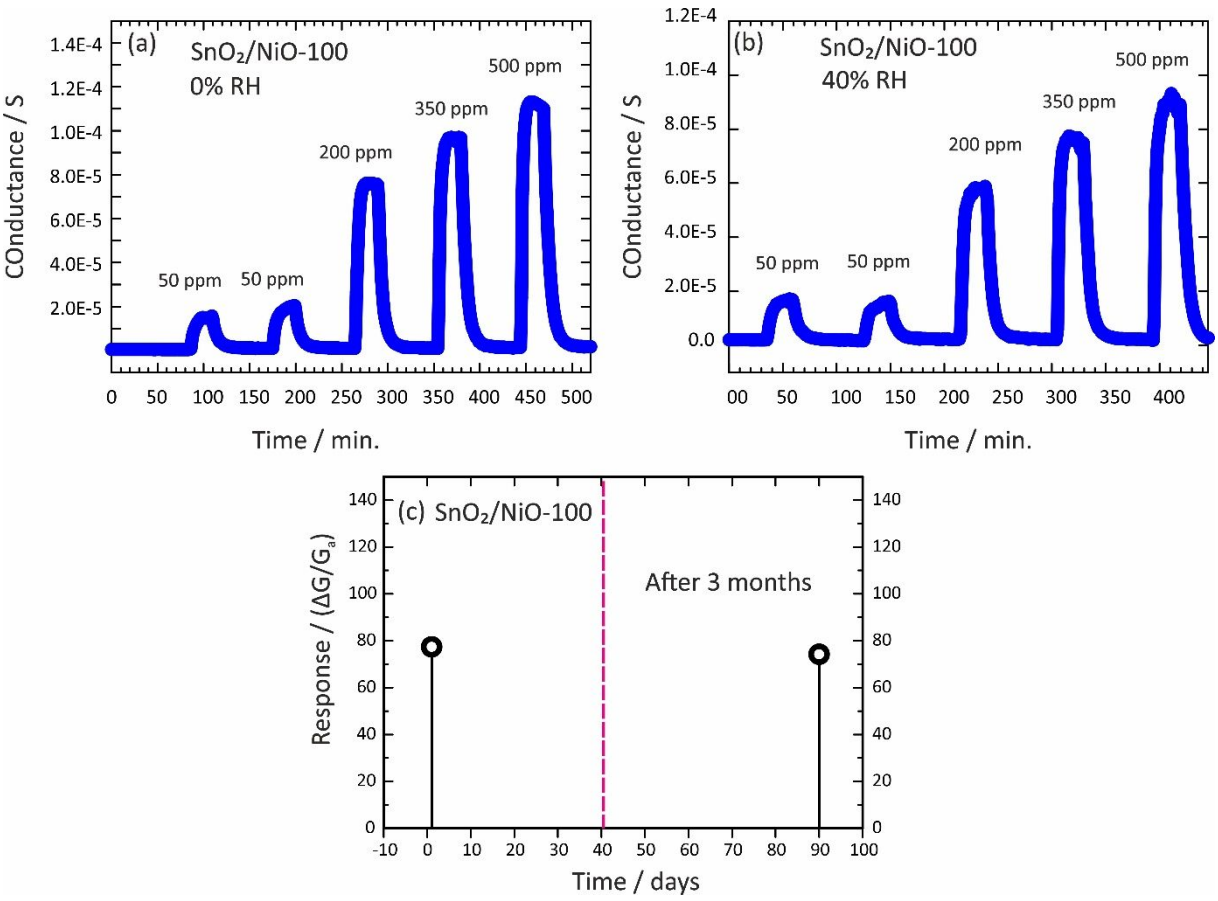

Figure S6. (a) The dynamic transient response for the SnO_2/NiO-*X* CSNWs sensor towards hydrogen at (a) 0% RH and (b) 40% RH, showing a repeatability of the signals (for 50 ppm of hydrogen) and a proportional increment in the response with respect to the analyte concentration.

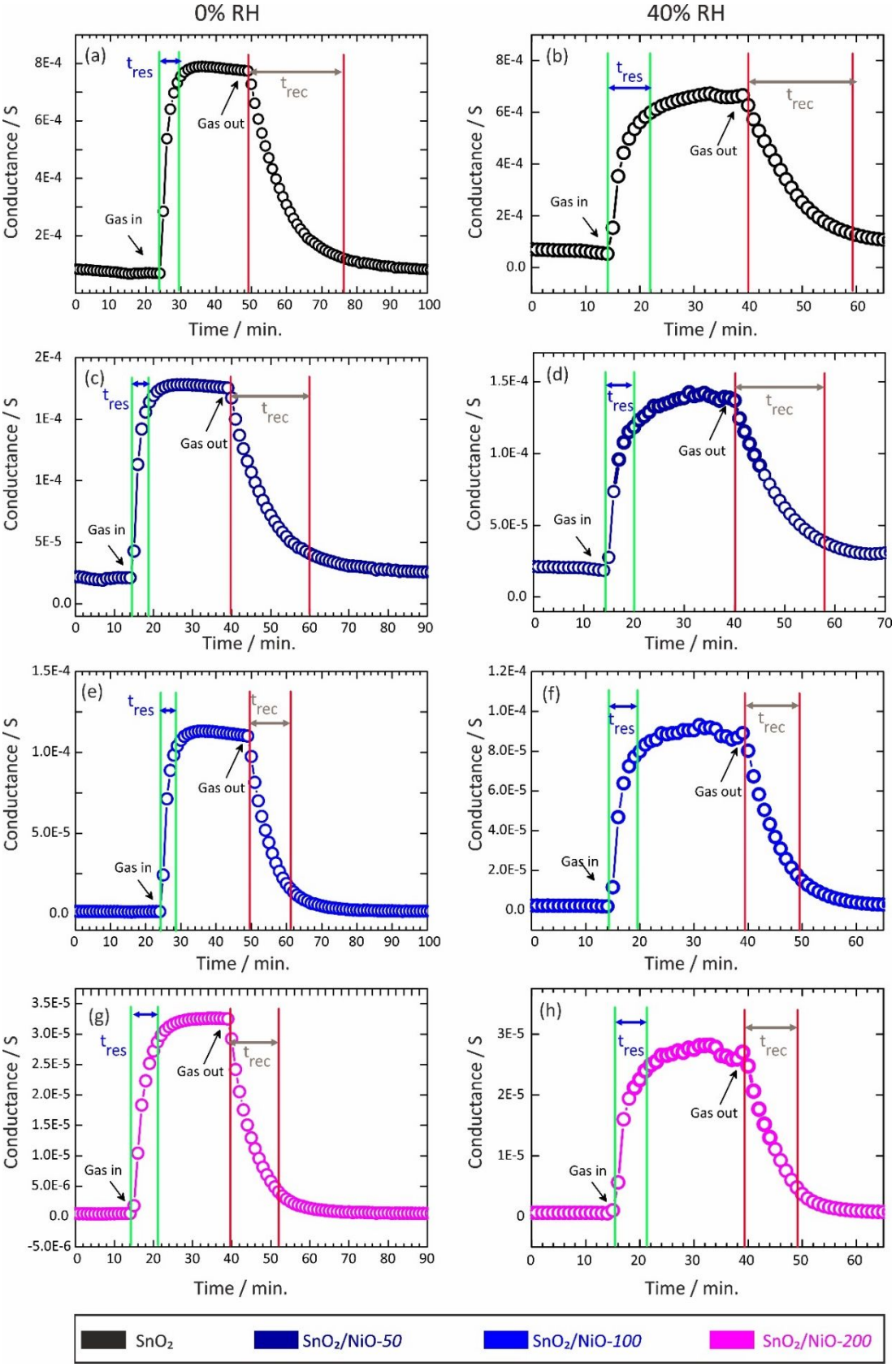

Figure S7. The response transient for the response time and recovery time of the SnO_2 NWs and SnO_2/NiO-*X* CSNWs towards hydrogen (500 ppm at 500 °C) at 0% RH (panel a, c, e, g) and at 40 % RH (panel b, d, f, h). The legends for all the panels are shown at the bottom.

Table S1. The response and recovery time of the SnO_2 NWS and SnO_2/NiO-*X* CSNWs towards hydrogen (500 ppm at 500 °C) at 0% RH and 40 % RH values conditions.

Sensors	0% RH		40 % RH	
	Response time (t_{res}) / minutes	Recovery time (t_{rec}) / minutes	Response time (t_{res}) / minutes	Recovery time (t_{rec}) / minutes
SnO_2	5	23	8	21
SnO_2/NiO-*50*	5	20	6	18
SnO_2/NiO-*100*	2	11	5	9
SnO_2/NiO-*200*	7	12	6	9

Table S2. Representative parameters and detection limits obtained by fitting of the calibration curve, Response = A $[C]^B$.

Sensors	**A**	**B**	**Detection limit**
SnO_2 NWs	0.95	0.53	1.1 ppm
SnO_2/NiO-50	0.76	0.47	1.8 ppm
SnO_2/NiO-200	0.15	1.00	6 ppm
SnO_2/NiO-*100* (RH 0%)	1.06	0.77	0.9 ppm
SnO_2/NiO-*100* (RH 40%)	0.51	0.72	2.5 ppm

1. McGahan, W. A.; Johs, B.; Woollam, J. A., Techniques for ellipsometric measurement of the thickness and optical constants of thin absorbing films. *Thin Solid Films* **1993,** *234* (1), 443-446.
2. Raza, M. H.; Movlaee, K.; Wu, Y.; El-Refaei, S. M.; Karg, M.; Leonardi, S. G.; Neri, G.; Pinna, N., Tuning the NiO Thin Film Morphology on Carbon Nanotubes by Atomic Layer Deposition for Enzyme-Free Glucose Sensing. *ChemElectroChem* **2019,** *6* (2), 383-392.
3. Fan, Y.; Wu, Y.; Clavel, G.; Raza, M. H.; Amsalem, P.; Koch, N.; Pinna, N., Optimization of the Activity of Ni-Based Nanostructures for the Oxygen Evolution Reaction. *ACS Appl. Energy Mater.* **2018,** *1* (9), 4554-4563.